Interaction of a rodlike charged macroparticle with a flowing plasma

S. V. Vladimirov*

Department of Theoretical Physics, School of Physics, The University of Sydney, New South Wales 2006, Australia

M. Nambu

Tokyo Metropolitan Institute of Technology, Asahigaoka, Tokyo 191-0065, Japan
(Received 29 January 2001; revised manuscript received 5 April 2001; published 18 July 2001)

The formation of the wake potential is demonstrated for a rodlike particle in a plasma with an ion flow. The cases of various charge distributions on the rod are studied, including those contributing to the dipole momentum, and different angles between the direction of the ion flow and the rod are considered. The possibilities of the formation of lattices composed of cylindrical macroparticles in a plasma are discussed.

I. INTRODUCTION

Most of the present dust-crystal experiments [1–4] involve dust particles levitating in the sheath region where strong ion flows are established. The ion flow naturally provides a distinctive direction, with plasma properties different in the direction parallel or perpendicular to the flow. This feature strongly influences formation of the plasma-dust crystals, with often observed feature of dust particle aligning in the direction of the flow [4].

A theory taking into account, that, asymmetry and suggesting that in the case of supersonic velocities of the flow the ion wake field is formed behind the levitating dust grain was proposed in Refs. [5,6]. The wake strongly affects interaction of dust particles in the direction of the ion flow, this was experimentally confirmed in Ref. [7]. Later, particle-in-cell simulations [8] demonstrated the formation of the wake potential whose wells can attract the lower dust grains. Recent three-dimensional (3D) molecular dynamic study [9] also shows the region of strong ion focusing behind the grain. According to the majority of the experiments, the most studied (theoretically, numerically, and experimentally) cases correspond to spherical dust grains.

Recent observations of the formation of plasma crystals composed of elongated particles [10] as well as communication [11] on the experiments with cylindrical particles levitating in the sheath of radio frequency (rf) discharge plasma prompted us to investigate the formation of the wake potential in the case of a rodlike charged particle. For simplicity, we do not study the effect of the charging of such type of particle, therefore just assuming that there is a given distribution of charges on the rod. We note that, in general, an inhomogeneous linear charge density distribution along the rod leads to the appearance of a dipole moment of a particle. The effect of the dipole moment on the wake formation of a pointlike particle was studied in [12]. However, the finite size of the rod affects the character of the wake, in particular, providing the additional degree of freedom connected with rotational inclination of the rod.

————

*Email address: S. Vladimirov@physics.usyd.edu.au; URL: http://www.physics.usyd.edu.au/~vladimi

Here, we would like to note, that this additional (rotational) degree of freedom will lead to new effects in experiments with cylindrical particles. Indeed, in the crystal lattices composed of a spherical particles, vibration modes associated with longitudinal [13] of transversal [14] (with respect to the propagation of the wave) motions of grains can be excited. The "liquid crystal" lattices composed of rods will have new rotational modes associated with their rotational motions, similar to those in liquid crystals. Excitation and interactions of all these modes introduce new phase transitions and affect those existing in lattices composed of spherical grains. As was pointed out recently [15], the wake can affect the interaction of the horizontal (longitudinal) and vertical (transverse) modes for spherical grains. Thus we expect that similar (or more complex) effects will exist for cylindrical particles, affecting their interaction and involving also the rotational modes. All this make the present study a necessary first step to understand the formation of "liquid crystal" lattices levitating in the sheath region where strong ion flows are established.

II. EQUATIONS FOR THE WAKE POTENTIAL

Consider the geometry sketched in Fig. 1. A finite size (in one direction) particle of the length d is immersed in an ion
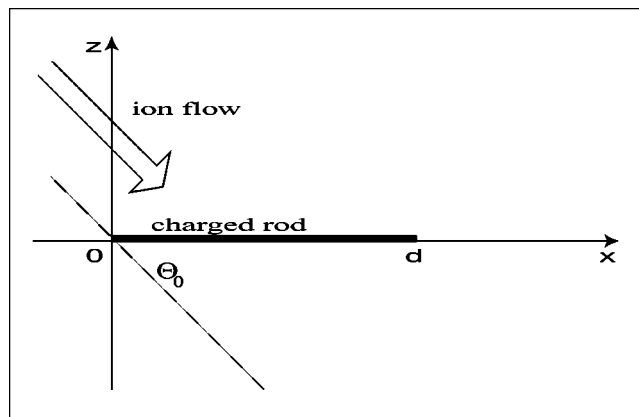

FIG. 1. Sketch of the considered geometry. The rod of the length d is assumed to be at the angle Θ_0 with respect to the direction of the ion flow.

flow of the speed $\mathbf{v}_0$. The angle between the direction of the flow and the rod is Θ_0. We choose the reference frame with the x axis along the rod, and the ion flow is in the xz plane, i.e., $\mathbf{v}_0 = (v_0 \cos \Theta_0, 0, -v_0 \sin \Theta_0)$. The y and z sizes of the particle are zero. The angle $\Theta_0 = \pi/2$ corresponds to the ion flow in (minus) z direction, perpendicular to the rod, and the angle $\Theta_0 = 0$ corresponds to the ion flow in x direction, parallel to the rod; note that in the experiments [11] both possibilities were observed. The three-dimensional charge density of such a particle is given by

$$\rho_d = \rho_l \delta(y) \delta(z), \tag{1}$$

where ρ_l is the linear density of the charge distribution on the rod. Below, we specify the following linear charge distributions: (a) charges distributed equally along the rod, $\rho_l = (Q_0/d) \theta(x) \theta(d-x)$; (b) charges distributed unequally along the rod, $\rho_l = (2Q_0 x/d^2) \theta(x) \theta(d-x)$; (c) charges distributed on the ends of the rod, $\rho_l = Q_1 \delta(x) + (Q_0 - Q_1) \delta(x-d)$. The total charge on the rod is Q_0 for all cases. Note that cases (b) and (c) correspond to the nonzero dipole moment of the rod: $P_0 = Q_0 d/6$ for the case (b), and $P_0 = (Q_0 - 2Q_1)d$ for the case (c) (we assume $Q_1 \neq Q_0/2$).

Poisson's equation for the Fourier transformed quantities is

$$\mathbf{k}^2 \varepsilon(\mathbf{k}, \omega) \Phi(\mathbf{k}, \omega) = 4\pi \rho_d(\mathbf{k}, \omega), \tag{2}$$

where the dielectric permittivity of a plasma in the presence of the ion flow is such that $|\mathbf{k}| v_{Ti} \ll |\omega - \mathbf{k} \cdot \mathbf{v}_0| \ll |\mathbf{k}| v_{Te}$ [here, $v_{Ti(e)} = (T_{i(e)}/m_{i(e)})^{1/2}$ is the ion (electron) thermal velocity, $T_{i(e)}$ is the ion (electron) temperature in energy units, and $m_{i(e)}$ is the ion (electron) mass] is given by

$$\varepsilon(\mathbf{k}, \omega) = 1 + \frac{1}{\mathbf{k}^2 \lambda_{De}^2} - \frac{\omega_{pi}^2}{(\omega - \mathbf{k} \cdot \mathbf{v}_0)^2}, \tag{3}$$

$\omega_{pi} = (4\pi n_i e^2/m_i)^{1/2}$ is the ion plasma frequency and $\lambda_{De} = (T_e/4\pi n_e e^2)^{1/2}$ is the electron Debye length. Furthermore, for the (stationary) particle charge density we have $\rho_d(\mathbf{k}, \omega) = 2\pi \rho_d(\mathbf{k}) \delta(\omega)$, where: (a) $\rho_d(\mathbf{k}) = iQ_0[\exp(-ik_x d) - 1]/k_x d$; (b) $\rho_d(\mathbf{k}) = 2Q_0[(1 + ik_x d)\exp(-ik_x d) - 1]/k_x^2 d^2$; (c) $\rho_d(\mathbf{k}) = Q_1 + (Q_0 - Q_1)\exp(-ik_x d)$.

Thus the electrostatic potential of such a particle can be written as

$$\Phi(\mathbf{r}, t) = \mathrm{Re} \int \frac{d\mathbf{k} \, d\omega}{4\pi^3 \mathbf{k}^2} \frac{\rho_d(\mathbf{k}, \omega) \exp(i\mathbf{k} \cdot \mathbf{r} - i\omega t)}{\varepsilon(\mathbf{k}, \omega)}. \tag{4}$$

For the static rod in the presence of the ion flow, the potential is given by

$$\Phi(\mathbf{r}) = \mathrm{Re} \int \frac{d\mathbf{k}}{2\pi^2 \mathbf{k}^2} \frac{\rho_d(\mathbf{k}) \exp(i\mathbf{k} \cdot \mathbf{r})}{\varepsilon(\mathbf{k}, -k_x v_0 \cos \Theta_0 + k_z v_0 \sin \Theta_0)}. \tag{5}$$

Separating in Eq. (5) the static Debye and the oscillating wake potentials $\Phi(\mathbf{r}) = \Phi_D(\mathbf{r}) + \Phi_W(\mathbf{r})$ [5,6], we have for $\Phi_W(\mathbf{r})$

$$\Phi_W(\mathbf{r}) = \mathrm{Re} \int \frac{d\mathbf{k}}{2\pi^2 \mathbf{k}^2} \frac{\rho_d(\mathbf{k}) \mathbf{k}^2 \lambda_{De}^2}{1 + \mathbf{k}^2 \lambda_{De}^2}$$
$$\times \frac{\omega_{\mathbf{k}}^2 \exp(i\mathbf{k} \cdot \mathbf{r})}{(-k_x v_0 \cos \Theta_0 + k_z v_0 \sin \Theta_0 + i0)^2 - \omega_{\mathbf{k}}^2}. \tag{6}$$

Here, $\omega_{\mathbf{k}} = |\mathbf{k}| v_s / (1 + \mathbf{k}^2 \lambda_{De}^2)^{1/2}$ is the characteristic frequency of the oscillations in the flow; it naturally appears when we equal to zero the plasma response function (3); $v_s = (T_e/m_i)^{1/2}$ is the ion sound speed. The potential (6) describes the strong resonant interaction between the oscillations in the ion flow and the test rod when $|k_x v_0 \cos \Theta_0 - k_z v_0 \sin \Theta_0|$ is close to the eigenfrequency $\omega_{\mathbf{k}}$ of the ion oscillations in the flow.

By rotating the wave number reference frame such that $k_x' = k_x \cos \Theta_0 - k_z \sin \Theta_0$ and $k_z' = k_x \sin \Theta_0 + k_z \cos \Theta_0$ (i.e., the ion flow is now in $-k_z'$ direction), we have from Eq. (6)

$$\Phi_W(\mathbf{r}) = \mathrm{Re} \int \frac{d\mathbf{k}'}{2\pi^2 \mathbf{k}'^2} \frac{\rho_d(\mathbf{k}') \mathbf{k}'^2 \lambda_{De}^2 \omega_{\mathbf{k}'}^2}{1 + \mathbf{k}'^2 \lambda_{De}^2}$$
$$\times \exp[ik_y y + ik_z'(x \sin \Theta_0 + z \cos \Theta_0)]$$
$$\times \frac{\exp[ik_x'(x \cos \Theta_0 - z \sin \Theta_0)]}{(k_x' - i0)^2 - \omega_{\mathbf{k}'}^2}, \tag{7}$$

where $d\mathbf{k}' = dk_x' dk_y dk_z'$, $\mathbf{k}'^2 = k_x'^2 + k_y^2 + k_z'^2$, and

(a) $\rho_d(\mathbf{k}') = (iQ_0/d)\{\exp[-id(k_x' \cos \Theta_0 + k_z' \sin \Theta_0)] - 1\}/(k_x' \cos \Theta_0 + k_z' \sin \Theta_0)$,

(b) $\rho_d(\mathbf{k}') = (2Q_0/d^2)\{[1 + i(k_x' \cos \Theta_0 + k_z' \sin \Theta_0)d]$
$\times \exp[-id(k_x' \cos \Theta_0 + k_z' \sin \Theta_0)] - 1\}/(k_x' \cos \Theta_0 + k_z' \sin \Theta_0)^2$,

(c) $\rho_d(\mathbf{k}') = Q_1 + (Q_0 - Q_1)\exp[-id(k_x' \cos \Theta_0 + k_z' \sin \Theta_0)]$.

Equation (7) can be integrated in k_x' by the standard way [5,6]. Taking into account only those poles corresponding to the ion-acoustic wake (other poles contribute to the Debye screening potential) and using for k_y and k_z', the dimensionless units normalized by the inverse of the Debye length, we find

$$\Phi_W(x \cos \Theta_0 - z \sin \Theta_0, \mathbf{r}_\perp)$$

$$= -\frac{Q_0}{\lambda_{De} M^2} \int_0^d \frac{d\tau}{d} A_d(\tau) \mathrm{Re} \int \frac{d\mathbf{k}_\perp}{2\pi |k_1|} \frac{k_\perp^2 + k_1^2}{k_0^2 + k_1^2}$$

$$\times \frac{\exp\{[ik_y y + ik_z'((x-\tau)\sin \Theta_0 + z \cos \Theta_0)]/\lambda_{De}\}}{1 + k_\perp^2 + k_1^2}$$

$$\times \sin\{k_1[(x-\tau)\cos \Theta_0 - z \sin \Theta_0]/\lambda_{De}\}. \qquad (8)$$

Here, $\mathbf{r}_\perp = (y, x \sin \Theta_0 + z \cos \Theta_0)$ is the radius vector in the plane, perpendicular to the ion flow, $\mathbf{k}_\perp = (k_y, k_z')$, $k_{0,1}^2 = \pm(1 - M^{-2} + k_\perp^2)/2 + [k_1^2 M^{-2} + (1 - M^{-2} + k_\perp^2)^2/4]^{1/2}$, and for the case (a) $A_d(\tau) = 1$, for the case (b) $A_d(\tau) = 2\tau/d$, and for the case (c) $A_d(\tau) = d(Q_1/Q_0)\delta(\tau) + d[1 - (Q_1/Q_0)]\delta(\tau - d)$. Physically, Eq. (8) corresponds to the sum of the wake potentials produced by the charges distributed on the rod; the integration in τ is the manifestation of this effect.

Integrating over the angles in the plane perpendicular to the direction of the ion flow, we obtain

$$\Phi_W(x \cos \Theta_0 - z \sin \Theta_0, \mathbf{r}_\perp)$$

$$= -\frac{Q_0}{\lambda_{De} M^2} \int_0^d \frac{d\tau}{d} A_d(\tau) \int_0^{+\infty} \frac{k_\perp dk_\perp}{|k_1|} \frac{k_\perp^2 + k_1^2}{k_0^2 + k_1^2}$$

$$\times \frac{J_0\{k_\perp \sqrt{y^2 + [(x-\tau)\sin \Theta_0 + z \cos \Theta_0]^2}/\lambda_{De}\}}{1 + k_\perp^2 + k_1^2}$$

$$\times \sin\{k_1[(x-\tau)\cos \Theta_0 - z \sin \Theta_0]/\lambda_{De}\}, \qquad (9)$$

where J_0 is the Bessel function of zero order.

III. APPROXIMATE ANALYTICAL EXPRESSIONS

The main contribution to the integral of Eq. (9) for $M \gg 1$, where $M = v_0/v_s$ is the Mach number of the ion flow, comes from $k_\perp \sim 1$ if $d < \lambda_{De}$; note that the latter is true for the present experiments, but, generally speaking, may not be the case in the future experiments. Then for distances $r_\perp = |\mathbf{r}_\perp| > \lambda_{De}$ and $|(x-\tau)\cos \Theta_0 - z \sin \Theta_0| > L_s$, where $L_s = \lambda_{De}\sqrt{M^2 - 1}$, we find the following approximate expression for the wake potential:

$$\Phi_W(x \cos \Theta_0 - z \sin \Theta_0, \mathbf{r}_\perp) \simeq \frac{Q_0}{1 - M^{-2}} \int_0^d \frac{d\tau}{d} A_d(\tau) \left[\frac{\lambda_{De}/2\pi}{\sqrt{y^2 + [(x-\tau)\sin \Theta_0 + z \cos \Theta_0]^2}} \right]^{1/2}$$

$$\times \left[\frac{\cos\{(\pi/4) + [x_-(\tau)/L_s]\}}{x_-(\tau)} + \frac{\cos\{(\pi/4) - [x_+(\tau)/L_s]\}}{x_+(\tau)} \right], \qquad (10)$$

where $x_\pm(\tau) = |(x-\tau)\cos \Theta_0 - z \sin \Theta_0| \pm \sqrt{M^2 - 1}\sqrt{y^2 + [(x-\tau)\sin \Theta_0 + z \cos \Theta_0]^2} > 0$ [we remind that the oscillating potential exists only in the wake cone of the test rod, i.e., for positive $x_\pm(\tau)$].

For small distances in the perpendicular direction, $r_\perp \ll \lambda_{De}$, and for the Mach number not near unity, $|(x-\tau)\cos \Theta_0 - z \sin \Theta_0| > L_s$, we assume $k_\perp^2 \ll (M^2 - 1)$ as well as $k_\perp \ll 1$, and obtain

$$\Phi_W(x \cos \Theta_0 - z \sin \Theta_0, \mathbf{r}_\perp) \simeq \frac{2Q_0}{L_s} \int_0^d \frac{d\tau}{d} A_d(\tau) \int_0^1 \frac{k_\perp^2 dk_\perp}{1 - M^{-2}} J_0\{k_\perp \sqrt{y^2 + [(x-\tau)\sin \Theta_0 + z \cos \Theta_0]^2}/\lambda_{De}\}$$

$$\times \sin\{k_1[(x-\tau)\cos \Theta_0 - z \sin \Theta_0]/\lambda_{De}\}. \qquad (11)$$

The main contribution to the stationary wake potential for $d \sin \Theta_0 < \lambda_{De}$ is now given by

$$\Phi_W(x \cos \Theta_0 - z \sin \Theta_0, r_\perp = 0) \approx \frac{2Q_0}{1 - M^{-2}} \int_0^d \frac{d\tau}{d} A_d(\tau) \frac{\cos\{[(x-\tau)\cos \Theta_0 - z \sin \Theta_0]/L_s\}}{|(x-\tau)\cos \Theta_0 - z \sin \Theta_0|}. \qquad (12)$$

Note that in the case $M \gg 1$ and smaller distances $|(x-\tau)\cos \Theta_0 - z \sin \Theta_0| < L_s$ (which can be realized for $d < L_s$), Eq. (11) gives the near-particle field ($M \gg 1$ asymptotics) $\Phi \sim Q_0[x - (d/2)]M^2/L_s^2 \sim Q_0[x - (d/2)]/\lambda_{De}^2 M^2$ for the case (a), and $\Phi \sim Q_0[(x/2) - (d/3)]M^2/L_s^2 \sim Q_0[(x/2) - (d/3)]/\lambda_{De}^2 M^2$ for the case (b). Furthermore, the upper limit for integration in Eq. (11), when $M \approx 1$, is $1 - M^{-2}$ [this follows from the general equation (9) and the expression for k_1], that for $|(x - d/2)\cos \Theta_0 - z \sin \Theta_0| > L_s$ gives $\Phi \sim \int_0^d (d\tau/d) A_d(\tau)\{Q_0/[(x-\tau)\cos \Theta_0 - z \sin \Theta_0]\}\cos\{[(x-\tau)\cos \Theta_0 - z \sin \Theta_0]/\lambda_{De}M\}$ and the scaling for the maximum potential [that can be estimated from $|(x - d/2)\cos \Theta_0 - z \sin \Theta_0| \sim L_s$] as $\Phi_{max} \sim \mathrm{const}/\sqrt{M^2 - 1}$.

For the case (c) we obtain from Eq. (10)

$$\Phi_W^{(c)}(x\cos\Theta_0 - z\sin\Theta_0, \mathbf{r}_\perp) \simeq \frac{Q_1}{1-M^{-2}} \left[\frac{\lambda_{De}/2\pi}{\sqrt{y^2 + (x\sin\Theta_0 + z\cos\Theta_0)^2}} \right]^{1/2} \left[\frac{\cos\{(\pi/4) + [x_-(0)/L_s]\}}{x_-(0)} \right.$$

$$\left. + \frac{\cos\{(\pi/4) - [x_+(0)/L_s]\}}{x_+(0)} \right] + \frac{Q_0 - Q_1}{1-M^{-2}} \left[\frac{\lambda_{De}/2\pi}{\sqrt{y^2 + [(x-d)\sin\Theta_0 + z\cos\Theta_0]^2}} \right]^{1/2}$$

$$\times \left[\frac{\cos\{(\pi/4) + [x_-(d)/L_s]\}}{x_-(d)} + \frac{\cos\{(\pi/4) - [x_+(d)/L_s]\}}{x_+(d)} \right]. \tag{13}$$

Equation (12) in this case will give us

$$\Phi_W(x\cos\Theta_0 - z\sin\Theta_0, r_\perp = 0) \approx \frac{2Q_1}{1-M^{-2}} \frac{\cos[(x\cos\Theta_0 - z\sin\Theta_0)/L_s]}{|x\cos\Theta_0 - z\sin\Theta_0|} + \frac{2(Q_0 - Q_1)}{1-M^{-2}} \frac{\cos\{[(x-d)\cos\Theta_0 - z\sin\Theta_0]/L_s\}}{|(x-d)\cos\Theta_0 - z\sin\Theta_0|}. \tag{14}$$

For the charge distributions (a) and (b), approximate expressions for the potential can be presented for the most important special cases $\Theta_0 = \pi$ and $\Theta_0 = -\pi/2$, i.e., when the rod is oriented along the flow and perpendicular to the ion flow, respectively. Note that this cases are of the most interest since current experiments demonstrate that $\Theta_0 = \pi$ and $\Theta_0 = -\pi/2$ correspond to the observed stable equilibrium positions of rods, e.g., see [11]. We have for $\Theta_0 = \pi$

$$\Phi_W(x, r_\perp = 0) \approx \frac{2Q_0}{1-M^{-2}} \int_0^d \frac{d\tau}{d} A_d(\tau) \frac{\cos[(x-\tau)/L_s]}{|(x-\tau)|}. \tag{15}$$

For $\Theta = -\pi/2$ if $d \ll \lambda_{De}$, we obtain a simple expression

$$\Phi_W(z, r_\perp = 0) \approx \frac{2Q_0}{1-M^{-2}} \frac{\cos[z/L_s]}{|z|}. \tag{16}$$

Note that this expression coincides in this limit with the wake field potential generated by a point charge [5].

IV. NUMERICAL RESULTS

The above approximate analytical expressions are not able to provide the character of the wake potential for the interesting cases when the rod length is of the order (or exceeds) the plasma Debye length. Thus in this section we present results of numerical integration of general equation (9) for the rod lengths $d_1 = \lambda_{De}/6 = 50$ μm, $d_2 = \lambda_{De} = 300$ μm, and $d_3 = 2\lambda_{De} = 600$ μm. The first case $d = d_1$ is interesting for comparison since the wake character in this case is practically close to that of a point charge.

Dependence of the wake field on the orientation of the rod with respect to the direction of the ion flow is the most pronounced for the flow velocities close to the speed of sound ($M \sim 1$), when the first maximum of the generated wake is close to the rod. We note that in general, the larger are the ion velocities, the stronger are ballistic effects in the ion focusing; this is because fewer ions participate in the wave-particle resonance, and the Mach cone is narrower. For

$M = 1.1$, we present in Fig. 2 the result of numerical integration of Eq. (9) for the case (a) (the surface plots for other cases look similar) and three orientations of the relatively long rod, $\Theta_0 = \pi, 5\pi/4, 3\pi/2$ (other parameters are: λ_{De}
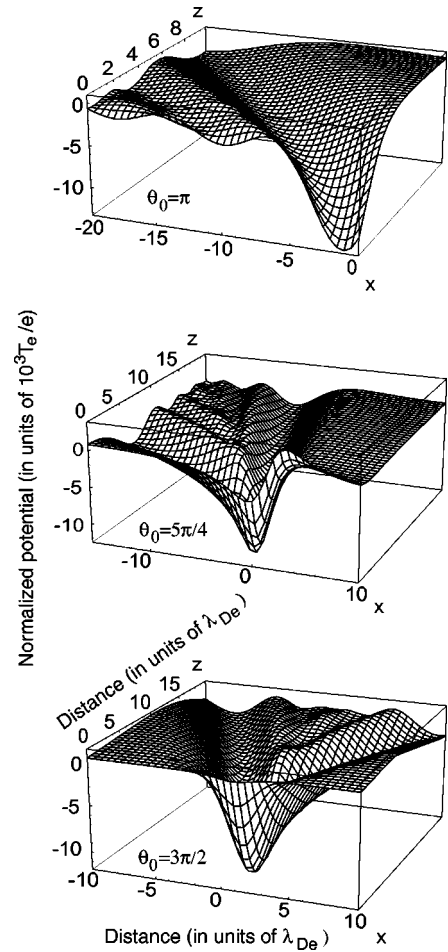

FIG. 2. The surface plot of the wake potentials for the case (a) and three different angles between the rod and the direction of the ion flow. Other parameters are $\lambda_{De} = 300$ μm, $T_e = 1$ eV, $M = 1.1$, $Q_0 = 5000e$.

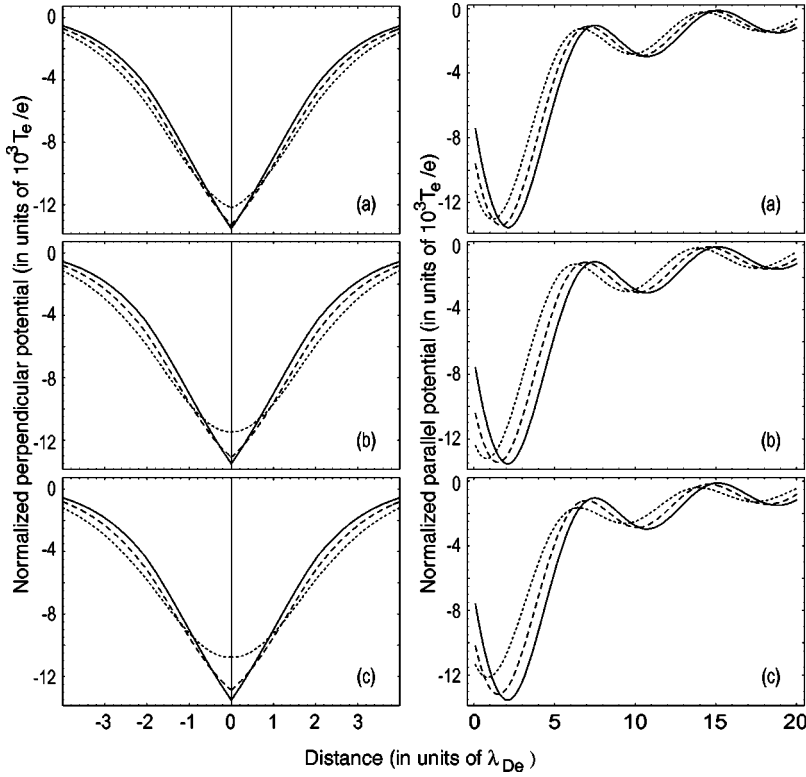FIG. 3. The wake potentials perpendicular and parallel to the ion flow for the cases (a)–(c), the angle $\Theta_0=\pi$ between the rod and the direction of the ion flow, and three different rod lengths: $d_1=\lambda_{De}/6=50$ μm (solid lines), $d_2=\lambda_{De}=300$ μm (dashed lines), and $d_3=2\lambda_{De}=600$ μm (dotted lines). Other parameters are $T_e=1$ eV, $M=1.1$, $Q_0=5000e$, and $Q_1=Q_0/3$.

$=300$ μm, $T_e=1$ eV, $M=1.1$, $Q_0=5000e$, and $Q_1=Q_0/3$ $=5000e/3)$. From these plots, we clearly see the wave character of the wake potential.

For better comparison of different cases and different rod lengths, we present on Figs. 3–5 the cross sections of the surface plots for the wake potential. Thus, Fig. 3 is the wake

potential in the directions perpendicular (left set of plots) and parallel to the ion flow (right set of plots) for the rod parallel to the ion flow, $\Theta=\pi$, and for the cases (a)–(c) for three different lengths of the rod, namely, $d_1=\lambda_{De}/6=50$ μm (solid line), $d_2=\lambda_{De}=300$ μm (dashed line), and $d_3=2\lambda_{De}=600$ μm (dotted line). The perpendicular wave po-

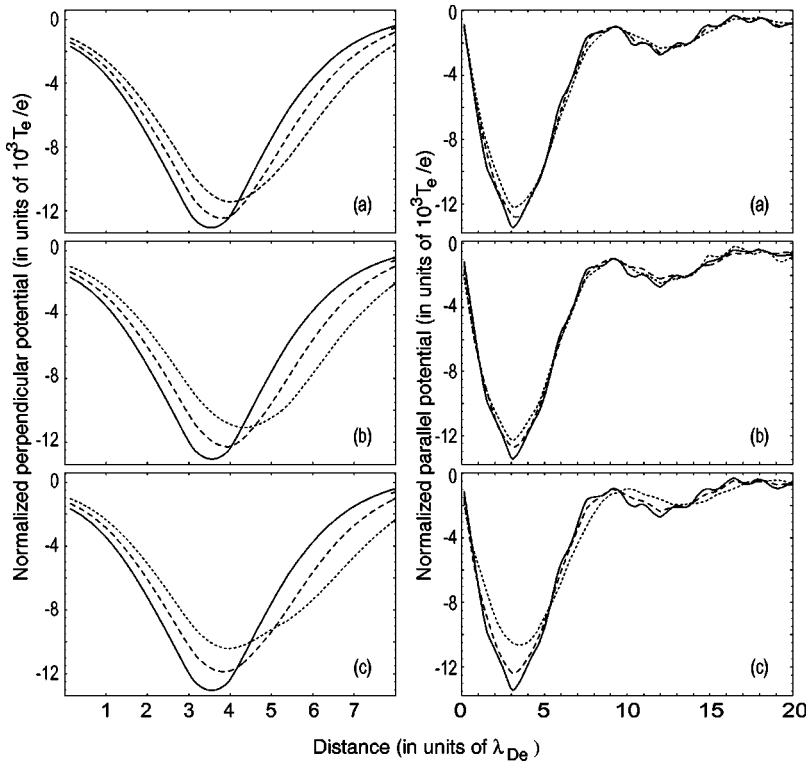

FIG. 4. The wake potentials perpendicular and parallel to the ion flow (and including the beginning of the reference frame $\mathbf{r}=0$) for the cases (a)–(c), the angle $\Theta_0=5\pi/4$ between the rod and the direction of the ion flow, and three different rod lengths: $d_1=\lambda_{De}/6=50$ μm (solid lines), $d_2=\lambda_{De}=300$ μm (dashed lines), and $d_3=2\lambda_{De}=600$ μm (dotted lines). Other parameters are $T_e=1$ eV, $M=1.1$, $Q_0=5000e$, and $Q_1=Q_0/3$.
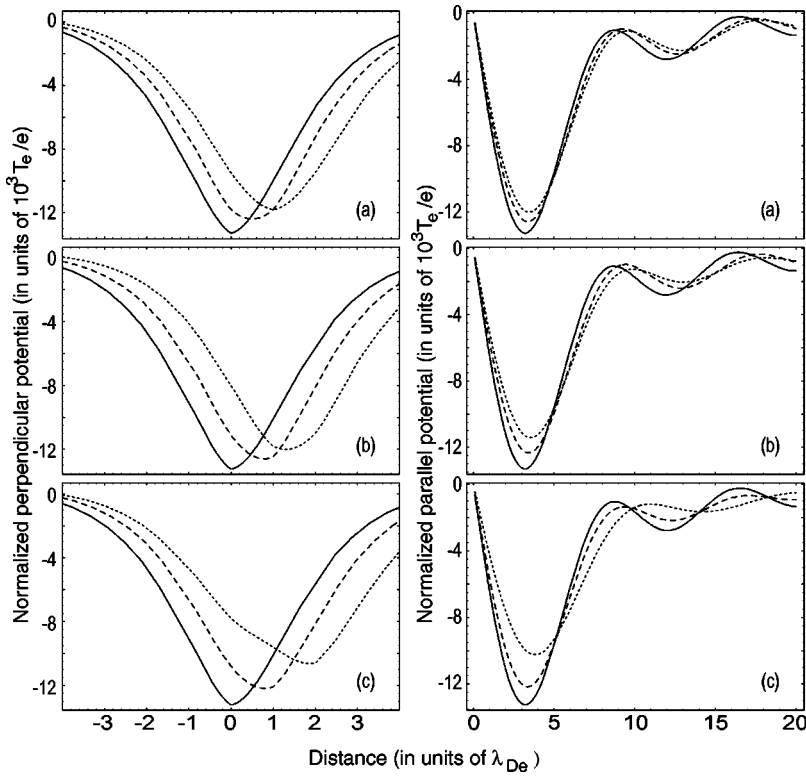
FIG. 5. The wake potentials perpendicular and parallel to the ion flow (and including the beginning of the reference frame $\mathbf{r}=0$) for the cases (a)–(c), the angle $\Theta_0=3\pi/2$ between the rod and the direction of the ion flow, and three different rod lengths: $d_1=\lambda_{De}/6=50$ μm (solid lines), $d_2=\lambda_{De}=300$ μm (dashed lines), and $d_3=2\lambda_{De}=600$ μm (dotted lines). Other parameters are $T_e=1$ eV, $M=1.1$, $Q_0=5000e$, and $Q_1=Q_0/3$.

tential is plotted along the line $x=-2\lambda_{De}$ (and parallel to the z axis), i.e., at the distance 600 μm from the (0,0) end of the rod [we remind the reader that the rod is at the coordinates $(0,0)-(d,0)$ in this case, cf. Fig. 1]. We note that the point $(-2\lambda_{De},0)$ approximately corresponds to the minimum of the wake potential, see the right set of plots of Fig. 3. We see that the minimum absolute value of the wake potential decreases and appears closer to the rod end with the increase of the rod length; on the other hand, the bigger is the charge separation along the length of the rod, the bigger is the difference between the location of the potential minima—compare the plots corresponding to the case (a) of the linear charge distribution along the rod and to the case (c) of (different) charges concentrated at the rod ends.

Figure 4 presents the character of the parallel and perpendicular wake potentials for the case $\Theta_0=5\pi/4$. The perpendicular potential is plotted along the line $(x,x+4.8\lambda_{De})$ (i.e., at the angle $-\pi/4$ to the x axis), which is shifted at the distance $4.8\lambda_{De}/\sqrt{2}\approx 3.4\lambda_{De}=1020$ μm from the (0,0) end of the rod, this distance approximately corresponds to the minimum of the wake potential in this case, see the right set of plots of the parallel wake potential on this figure. The parallel wake potential is plotted along the line $(x-d/2,x)$, where $d=d_1=\lambda_{De}/6=50$ μm (solid line), $d=d_2=\lambda_{De}=300$ μm (dashed line), and $d=d_3=2\lambda_{De}=600$ μm (dotted line), i.e., the line crossing the rod at the angle $-\pi/4$ in its middle. Here, we can see the qualitative difference with the previous case of the rod parallel to the ion flow, namely, the location of the minimum of the potential in the direction along the flow is practically independent of the rod length as well as of the charge distribution along the rod, see the right set of plots on this figure. On the contrary, the location of the minimum of the potential in the direction, perpendicular to

the flow changes with the rod length as well as with the charge distribution on the rod, see the left set of plots. The value of the absolute minimum of the wake potential in this case depends on the rod length similarly to the previous case: the potential is more shallow for longer rods, also acquiring the slightly asymmetric character for the asymmetric charge distribution along the rod, see the dotted curve, case (c), on the left set of plots of Fig. 4.

The character of the parallel and perpendicular wake potentials for the case $\Theta_0=3\pi/2$, i.e., for the rod oriented perpendicular to the ion flow, is presented on Fig. 5. The perpendicular potential is plotted along the line $z=3.5\lambda_{De}$ (i.e., at the angle $\pi/2$ to the z axis, parallel to the x axis), which is therefore shifted at the distance 1050 μm from the rod; this distance approximately corresponds to the minimum of the wake potential in this case, see the right set of plots of the parallel wake potential on this figure. The parallel wake potential is plotted along the line $x=2d/3$, where $d=d_1=\lambda_{De}/6=50$ μm (solid line), $d=d_2=\lambda_{De}=300$ μm (dashed line), and $d=d_3=2\lambda_{De}=600$ μm (dotted line), i.e., the line crossing the rod at the angle $\pi/2$ in the point $(2d/3,0)$. Here, the qualitative features appeared in the previous case (see Fig. 4), are more pronounced, namely: the location of the minimum of the potential in the direction along the flow is almost independent of the rod length with small charge difference along the rod, see cases (a) and (b) of the right set of plots on this figure. On the other hand, the new feature for the rod with the big charge separation, case (c), is that the minimum of the wake potential is further away from the rod for the bigger rod length. Note that this behavior is opposite to the dependence of the location of the potential minimum on the rod length for the rod oriented parallel to the flow, cf. Fig. 3. The location of the minimum of

the potential in the direction, perpendicular to the flow, clearly changes with the rod length as well as with the charge distribution on the rod, see the left set of plots. The value of the absolute minimum of the wake potential in this case depends on the rod length similar to the previous cases: the potential is shallower for longer rods, having the clear asymmetric character for the asymmetric charge distribution along the rod, see the dotted curve, case (c) on the left set of plots of Fig. 5.

Overall, we see that the more is the angle between the rod and the direction of the flow, the closer is the first maximum of the wake potential to the rod. We note that this type of behavior is more pronounced for longer rods with the big charge separation. Physically, it is clear that the shorter is the rod length, the closer is the character of the wake potential to that of a point charge.

V. CONCLUSIONS

To conclude, we studied the formation of the wake potential for a rodlike particle with distributed charges. We demonstrated that the basic feature of the wake in the case of supersonic velocities of the ion flow, namely, its oscillating character, first reported for spherical particles, takes also place for the rods. The longer are the rods, the more is the difference in the characteristics of the wake potential as functions of the rod lengths and/or charge distribution along the rod. Regarding the formation of the wake potentials of rodlike particles, the plasma electron Debye length is the most important characteristic scale: for rods much shorter than the Debye length, the wake potential is practically the same as for the point particles; on the other hand, for rod lengths comparable or exceeding the Debye length, the characteristics of the wake potential develop dependence on the orientation of the rod with respect to the ion flow as well as on the character of the charge distribution along the rod. The actual difference, e.g., for the location of the potential first minimum in the case of long (of the order of or exceeding the plasma electron Debye length) rods with large charge separation can be of the order of the electron Debye lengths, i.e., of order half a millimeter for the typical discharge parameters that is an easy detectable effect in the laboratory. The presented results are important for the present and planning experiments involving cylindrical particles. Furthermore, oscillations of rods as well as specific lattice modes propagating in the "liquid plasma" crystals, will be affected by the wake. Indeed, for the rotationally oscillating (in the plane parallel to the ion flow, i.e., in the vertical plane in the experiment) rods the motion of the wake potential minimum will take place thus strongly influencing the location of the downstream particles as well as the vertical arrangements and the vibration modes in the downstream chains. This is a fruitful field for further research.

[1] H. M. Thomas *et al.*, Phys. Rev. Lett. **73**, 652 (1994).

[2] A. Melzer, T. Trottenberg, and A. Piel, Phys. Lett. A **191**, 301 (1994).

[3] J. H. Chu and Lin I, Physica A **205**, 183 (1994).

[4] H. M. Thomas and G. E. Morfill, Nature (London) **379**, 806 (1996).

[5] S. V. Vladimirov and M. Nambu, Phys. Rev. E **52**, 2172 (1995).

[6] S. V. Vladimirov and O. Ishihara, Phys. Plasmas **3**, 444 (1996); O. Ishihara and S. V. Vladimirov, *ibid.* **4**, 69 (1997).

[7] K. Takahashi, T. Oishi, K. I. Shimonai, Y. Hayashi, and S. Nishimo, Phys. Rev. E **58**, 7805 (1998).

[8] D. Winske, W. Daughton, D. S. Lemons, and M. S. Murillo, Phys. Plasmas **7**, 2320 (2000).

[9] S. A. Maiorov, S. V. Vladimirov, and N. F. Cramer, Phys. Rev. E **63**, 017401 (2001).

[10] U. Mohideen, H. U. Rahman, M. A. Smith, M. Rosenberg, and D. A. Mendis, Phys. Rev. Lett. **81**, 349 (1998).

[11] B. M. Annaratone, A. G. Khrapak, A. V. Ivlev, G. Söllner, P. Bryant, R. Sütterlin, U. Konopka, K. Yoshino, M. Zuzic, H. M. Thomas, and G. E. Morfill, Phys. Rev. E **63**, 036406 (2001).

[12] O. Ishihara, S. V. Vladimirov, and N. F. Cramer, Phys. Rev. E **61**, 7246 (2000).

[13] F. Melandsø, Phys. Plasmas **3**, 3890 (1996).

[14] S. V. Vladimirov, P. V. Shevchenko, and N. F. Cramer, Phys. Rev. E **56**, 74 (1997).

[15] A. V. Ivlev and G. Morfill, Phys. Rev. E **63**, 016409 (2001).